

materiais para preparar as outras seis soluções de pH de referência. (1)

Verificou-se que o dihidrogeno citrato de potássio, de diversas fontes comerciais, é acompanhada de ácido cítrico, em maior ou menor quantidade, como resultado do processo de síntese. (3)

Foi desenvolvido um processo para a extracção do ácido cítrico (4) dado que a sua presença conduz a abaixamento do valor de pH do tampão. A sua remoção não resolve completamente o problema, dado que surgem valores acima dos previstos. Estes são resultado da presença de contaminantes de outra natureza, que duplamente contribuem para esse efeito. Por um lado a sua presença origina soluções de dihidrogeno citrato de potássio mais diluídas, por outro lado poderão as próprias espécies existentes, ou novas espécies originadas no processo de extracção, apresentar características mais básicas.

Neste trabalho identificam-se as referidas situações e estabelece-se uma metodologia que permite a obtenção do dihidrogeno citrato de potássio em elevadas condições de pureza, permitindo eventualmente a sua promoção a material de referência. Pela sua aplicação são produzidas soluções tampão padrão citrato de pH de referência, o que se comprova pela avaliação de valores de f.e.m. de células de Harned concordantes com valores já estabelecidos para o produto sintetizado. (1,3)

- (1) R.G. Bates, Critical Reviews in Analytical Chemistry, 10, 248 (1981).
- (2) B.R. Staples and R.G. Bates, J. Res. N.B.S., 73A, 37 (1969).
- (3) R.G. Bates and Gladys D. Pinching, J. Am. Chem. Soc., 71, 1274 (1949).
- (4) M. Filomena G.F.C. Camões e M.J. Guiomar H.M. Lito, Comunicação apresentada a "Euroanalysis VI", Setembro 1987 - Paris.

ELECTROCHEMICAL BEHAVIOR OF A Cu-Ag-Al ALLOY. I. POTENTIODYNAMIC STUDIES IN SODIUM HYDROXIDE.

Roberto Z. Nakazato (*), Paulo T.A. Sumodjo (**), & Assis V. Benedetti(*)

(*) Instituto de Química da Universidade Estadual Paulista, C.P. 174, 14.800 - Araraquara, São Paulo - Brasil

(**) Instituto de Química da Universidade de São Paulo, C.P. 20.780, 01498 - São Paulo, SP - Brasil.

Copper-Silver-Aluminium alloys have some practical interest, mainly in electronics and dentistry. It is thus worthwhile to study the stability and passivation of the material in different media. In this communication the potentiodynamic behavior of the alloy in alkaline media is discussed.

Experimental

The electrolysis cell consisted of a conventional three-electrode arrangement. The working electrode was a disc of the alloy (79.5% Cu, 10.5% Al, 10.0% Ag), apparent area 0.049 cm^2 . The counter electrode was a platinum sheet and a reversible hydrogen electrode in the same solution (RHE) was used as a reference electrode. NaOH 0.5 M, prepared from sodium hydroxide AR grade and triply distilled water, was employed as electrolyte. The working electrode was mechanically polished before immersion in the air-free electrolyte. The experiments were run at 30°C .

Results and Discussion

The n^{th} sweep cyclic voltammogram run between -0.5 V and 1.7 V at 0.10 V.s^{-1} (Fig. 1) shows a multiplicity of anodic and cathodic current peaks. The characteristics of the current peaks depend on variables such as the number of initial potential cycles, the switching potentials and the rate of potential perturbation. A comparison of the resulting potentiodynamic I/E profiles with the corresponding obtained with the pure metals show that peak current A_2 is related to the oxida-

tion of metallic copper to Cu^{I} , which undergo further oxidation to Cu^{II} , peak A_3 . The oxidation of metallic silver to Ag^{I} occurs in the potential corresponding to A_4 . A_5 is a complex current peak involving the pairs $\text{Ag}^{\text{I}} \rightarrow \text{Ag}^{\text{II}}$ and $\text{Cu}^{\text{II}} \rightarrow \text{Cu}^{\text{III}}$. C_6 may be attributed to the reduction of Cu^{III} , C_7 and C_8 , to the silver reduction processes and finally, C_9 , C_{10} and C_{11} are related to copper species reduction.

Figure 2 illustrates the voltammograms run between 0.15 V and 0.75 V potential range, involving Cu^{O} and Cu^{I} species, for different potential sweep rates, v . As it can be seen, A_2 shows a multiplicity of current peaks at low v , indicating that the process is a complex one, probably involving the ageing of Cu^{I} surface species. The ratio Q_a/Q_c , of the charges under the anodic and cathodic peaks, is close to 1, independently of v . The linear relationships observed in Figures 3 & 4 are predicted by the theory of film formation controlled by the surface reaction [S.Srinivasan & E. Gileadi, *Electrochim. Acta*, 11, 321(1966)].

In the 1.2 V and 1.7 V potential range, corresponding to the $\text{Ag}^{\text{I}}|\text{Ag}^{\text{I}}$ process, the voltammograms at different v exhibit one anodic current peak and the corresponding cathodic current peak (Fig. 5). One observes that the height of A_5 and C_7 increases as v increases, and the corresponding current peak potentials shift towards the positive and negative direction, respectively. The ratio Q_a/Q_c , of the charges under the anodic A_5 and corresponding cathodic peak C_7 , is > 1 for $v > 25$ mV/s, indicating that a dissolution/precipitation process possibly occurs. The resulting linear relationships I_p vs $v^{1/2}$ and E_p vs $v^{1/2}$ suggest that the process is controlled via the pore resistance mechanism [D.D. MacDonald, "Transient Techniques in Electrochemistry", Plenum Press, New York, 1977, chap. 8.].

In the potential range investigated it was not observed any influence of the aluminium.

Acknowledgment

The authors thank the financial support from FAPESP and CAPES.

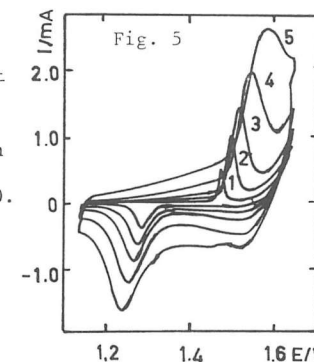
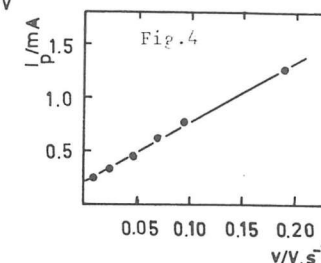
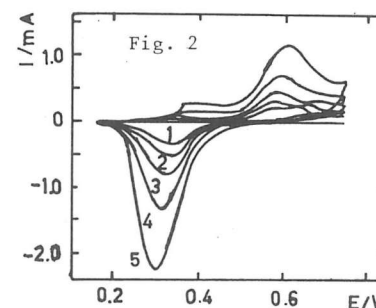
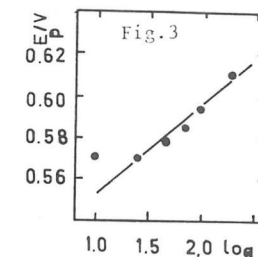
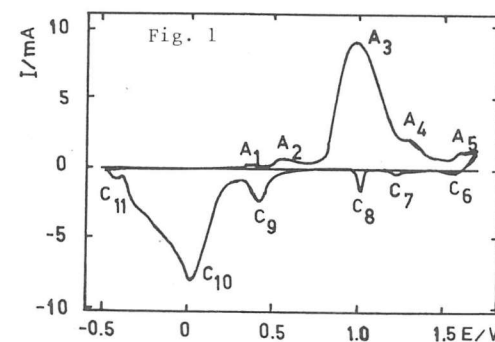


Fig.1. Stabilized potentiodynamic I/E profile at 0.1 V/s; 0.5 M NaOH; 30°C. Electrode area = 0.049 cm².

Fig.2. Cyclic voltammograms for $\text{Cu}^{\text{I}}|\text{Cu}^{\text{O}}$ run at different potential sweep rates (mV/s): (1) 10; (2) 25; (3) 50; (4) 100 and (5) 200.

Fig.3. I_p^a vs. v

Fig.4. E_p^a vs. $\log v$.

Fig.5. Potentiodynamic I/E profiles for $\text{Ag}^{\text{I}}|\text{Ag}^{\text{I}}$ obtained for different potential sweep rates (mV/s): (1) 10; (2) 25; (3) 50; (4) 100; (5) 200.